

Development and Interfacial Characterization of Co/Mg Periodic Multilayers for the EUV Range

K. Le Guen,* M.-H. Hu, J.-M. André, and P. Jonnard

Laboratoire Chimie Physique - Matière Rayonnement, University Pierre et Marie Curie Paris 06, CNRS UMR 7614, 11 rue Pierre et Marie Curie, F-75231 Paris cedex 05, France

S. K. Zhou, H. Ch. Li, J. T. Zhu, and Z. S. Wang

Institute of Precision Optical Engineering, Department of Physics, Tongji University, Shanghai 200092, People's Republic of China

C. Meny

Institut de Physique et Chimie des Matériaux de Strasbourg, CNRS UMR 7504, 23 rue du Loess, BP 43, F-67034 Strasbourg cedex 2, France

Received: November 23, 2009; Revised Manuscript Received: February 3, 2010

We propose a new system, namely the periodic Co/Mg multilayer system, for optics applications in the EUV range. Close to the Mg L edge, i.e., around a wavelength of 25 nm or a photon energy of 50 eV, a reflectivity of about 43% is measured at 45° for s-polarized radiation. Moreover, it appears that this system is stable over a period of time of three months. The introduction of thin boron carbide interfacial layers proves disastrous contrary to simulations that show this could be beneficial. We combine X-ray reflectivity in the hard X-ray range, X-ray emission spectroscopy, and nuclear magnetic resonance to determine the thickness and roughness of the Co and Mg layers as well as the chemical state of the Co and Mg atoms at the interfaces. This reveals that in the Co/Mg system the interfaces are abrupt and there is no interdiffusion between the Co and Mg layers. Then the difference between the experimental and simulated reflectivities is ascribed to the interfacial roughness of the order of 0.4 nm. In the Co/Mg/B₄C system, evidence of a large mixing of the Co and B₄C layers is presented and explains the poor reflectance of this system.

1. Introduction

Periodic multilayers made of alternating nanometric thin films nowadays play an important role for optical applications from the extreme ultraviolet (EUV) to the hard X-rays.^{1,2} The performances of these structures in terms of reflectance and bandwidth strongly depend on the quality of interfaces between the different layers, i.e. the value of the interfacial roughness and the interdiffusion. Thus the development of optimized stacks relies on the characterization of the layers, determination of their thickness, roughness, and density, as well as the comprehension of the interfacial phenomena, atomic diffusion, or formation of compounds.

In this paper we propose a new system, namely Co/Mg, for applications in the EUV range close to the Mg L edge, that is to say around 25 nm wavelength or 50 eV photon energy. In view of a possible application as monochromator, the simulated reflectivity obtained with the IMD software³ and assuming an s-polarized light incoming at 45° is calculated. It shows a maximum of 56.5% given an “ideal” multilayer with no interaction between the layers and no interfacial roughness.⁴ Because we suspect a possible interdiffusion and the formation of compounds at the metal–metal interfaces, we consider the introduction of boron carbide at one interface. This kind of barrier layer has proved its efficiency for numerous multilayer

systems devoted to optics applications.^{5,6} For the ideal Co/Mg/B₄C multilayer a maximum reflectance of 53.5% is calculated.⁴

For comparison, in the case of the Mg/SiC system, simulations of an “ideal” multilayer indicate a reflectance of about 60% at 30.4 nm and 20° off normal incidence using s-polarized light. But, reflectivity measurements at 30.4 nm demonstrate that the large value of the rms interfacial roughness (≥ 1 nm) is directly responsible for the limitation of the optical performances (R is only 40%).⁷ This example has motivated us to explore other optimum material combinations, even systems where simulations predict a reflectance slightly lower than that of Mg/SiC provided that (i) the measured roughness remains moderate and (ii), as a consequence, the discrepancy between simulated and measured reflectance values is lower than in the case of Mg/SiC. Indeed, at 30.4 nm and near normal incidence, the Co/Mg system gives experimental performances of the same order of magnitude as the Mg/SiC system: 40% reflectivity and 1.3 nm bandwidth for Co/Mg; 45% reflectivity and 1.7 nm bandwidth for Mg/SiC.⁸ In the same conditions, the Al/SiC and Mo/Si systems reach reflectance of only 17% and 22%, respectively,⁹ and B₄C/Mo/Si reaches 32%.¹⁰

Multilayers are fabricated by magnetron sputtering and tested in the EUV range. They are characterized by X-ray reflectivity (XRR) in the hard X-ray range after their preparation to determine the thickness, roughness, and density of their layers. The introduction of thin boron carbide layers is also considered. The time stability of these structures is also studied over a duration of about 3 months. To determine if some interaction

* To whom correspondence should be addressed. Phone: 33 1 44 27 66 08. Fax: 33 1 44 27 62 26. E-mail: karine.le_guen@upmc.fr.

TABLE 1: Designed Structure of the Co/Mg and Co/Mg/B₄C Multilayers

multilayer	sample name	period d (nm)	d_{Co} (nm)	d_{Mg} (nm)	$d_{\text{B}_4\text{C}}$ (nm)	simulated reflectivity
Co/Mg	CoMg_1	8.00	2.55	5.45	—	—
	CoMg_2	17.00	2.55	14.45	—	56.5% @ 25.2 nm
Co/Mg/B ₄ C	CoMgB ₄ C_1	8.90	2.55	5.45	0.90	—
	CoMgB ₄ C_2	17.90	2.55	14.45	0.90	53.5% @ 25.8 nm

takes place between the layers, we look to the chemical state of the Mg and Co atoms present within the multilayer, by using X-ray emission spectroscopy (XES) and nuclear magnetic resonance (NMR). If there is some interdiffusion between the layers, the chemical state of the atoms of the interfacial layer is different from that of the atoms at the center of the layer. In this case, at least two chemical states of Mg and Co should be observed. The interest of combining XES and NMR is to obtain the information from both sides of the interface.

2. Experimental Section

2.1. Sample Preparation. The studied periodic Co/Mg and Co/Mg/B₄C multilayers were prepared by using a calibrated ultrahigh vacuum direct current magnetron sputtering system (JGP560C6, SKY Inc., China) with targets of Co (purity 99.95%), Mg (purity 99.98%), and B₄C (purity 99.5%) in Ar gas (99.999%). The targets are 100 mm in diameter. The base pressure was 10^{-4} Pa and the working pressure was 0.13 Pa of Ar gas. The power applied on the Co, Mg, and B₄C targets was set to 25, 15, and 80 W, respectively. The multilayers were all deposited onto 30 mm × 30 mm ultrasmooth polished Si substrates with rms surface roughness of 0.3 nm.

The description of the designed structure of each multilayered sample is summarized in Table 1. Each sample is made of 30 bilayers. The first layer on the substrate is the cobalt one. A 3.50-nm-thick capping layer made of B₄C is deposited at the surface of each sample in order to prevent oxidation: in the sample where 0.90-nm-thick B₄C layers enter in the composition of the periodic structure, the thickness of the capping layer is reduced to 2.60 nm.

The samples named CoMg_1 and CoMgB₄C_1, both characterized by a short period (8.00 and 8.90 nm, respectively), are dedicated to the X-ray emission spectroscopy analysis. Indeed, to be able to identify by means of XES the formation of an interfacial layer at the interface between two successive layers, the thickness of this interfacial layer should be comparable to that of the layer of the emitting atoms (Co layer for the Co L $\alpha\beta$ emissions and Mg layer for the Mg K β emission). The two remaining samples (namely CoMg_2 and CoMgB₄C_2) are designed to lead to the highest reflectivity value at the application wavelength. Thus, these two samples are analyzed by means of XRR in the EUV range. Moreover, the four samples have been studied by NMR spectroscopy in order to study the chemical state of the (magnetic) Co atoms.

2.2. X-ray Reflectivity at 0.154 nm. The structural quality of all these multilayers and the agreement between the aimed and effective thicknesses have been checked by using X-ray reflectivity at 0.154 nm (Cu K α emission at 8048 eV). The measurements are made with use of a grazing incidence X-ray reflectometer (D1 system, Bede Ltd.) working in the θ - 2θ mode. The angular resolution is 5/1000°. Bragg law corrected for refraction was used to determine the multilayer period. The fit of the XRR curves performed with Bede Refs software (genetic algorithm)¹¹ was used to determine individual layer thickness, roughness, and layer density.

2.3. EUV Reflectivity. The measurement of the reflectivity curves in the EUV domain is performed on the BEAR

beamline¹² at the Elettra synchrotron center using s-polarization. The photon energy is carefully calibrated by using the Pt 4f_{7/2} feature and the Si L edge. The goniometer angular resolution is 1/100°. Impinging and reflected photon intensities are measured by using a solid state photodiode. Incident intensities are monitored with an Au mesh inserted in the beam path whose drain current is used for normalization. The overall accuracy on the absolute reflectivity values is estimated to be about 1%.

2.4. X-ray Emission Spectroscopy. The X-ray emission analysis is performed in a high-resolution wavelength dispersive soft X-ray spectrometer.¹³ The Mg K β and Co L $\alpha\beta$ emission coming from the magnesium and cobalt atoms present in the Co/Mg and Co/Mg/B₄C multilayered samples are analyzed. These emissions correspond to the Mg 3p-1s and Co 3d-2p_{3/2} and 3d-2p_{1/2} transitions respectively and are related to the occupied valence states having the Mg 3p and Co 3d character. These emissions are sensitive to the physicochemical state of the magnesium and cobalt atoms, respectively.^{7,14}

The Mg 1s and Co 2p core holes are created by an electron beam coming from a Pierce gun. The energy of the incident electrons was chosen to be higher than the threshold of the studied emission (1303.4 and 778.8 eV for the Mg 1s and Co 2p_{3/2} binding energies, respectively). In the present case, the electron energy was 7.5 keV for the Mg K β emission and 3.5 keV for the Co L $\alpha\beta$ emissions. Following the ionization of the atoms present in the sample, characteristic X-rays are emitted,^{15,16} then dispersed by a (10 $\bar{1}0$) beryl (for Mg K β emission) or TIAP (001) (for Co L $\alpha\beta$ emission) bent crystal and detected in a gas-flux counter working in the Geiger regime. The current density of the electrons reaching the sample is set to less than 1 mA·cm⁻² to ensure that the shape and intensity of the studied emission remain constant throughout the measurements.

In the following, each presented emission spectrum is normalized with respect to its maximum and a linear background corresponding to the Bremsstrahlung contribution is subtracted. To determine the composition of the multilayers (especially to identify possible interfacial compounds), their emission spectrum is compared to that of reference compounds. This methodology is now routinely used to study complex materials.^{6,17-24}

In the Co-C binary phase diagram, no compound arising from the reaction of the two materials is mentioned.²⁵ The region for the solubility of graphite in cobalt is limited to the 0-1% C range. On the contrary, the Co-B and Co-Mg binary phase diagrams exhibit the Co₃B, Co₂B, and CoB²⁷ and MgCo₂²⁷ compounds, respectively. In the Mg-B binary phase diagram, the MgB₂, MgB₄, and MgB₇ compounds are reported.²⁸ To our knowledge, the Co-B-C ternary diagram is not available in the literature. Among all these compounds, only MgB₂ was easily available: its Mg K β emission spectrum will be compared to that of the Co/Mg/B₄C multilayer. For the same emission, we have also considered as references a MgO single crystal cleaved along the (100) plane and a MgZn (Zn 1 wt %) dilute alloy. For that latter sample, we have carefully checked that its Mg K β emission spectrum is very close to that of the Mg metal.²⁹ In the case of the Co L $\alpha\beta$ emissions, a Co thin film deposited by magnetron sputtering is used as reference.

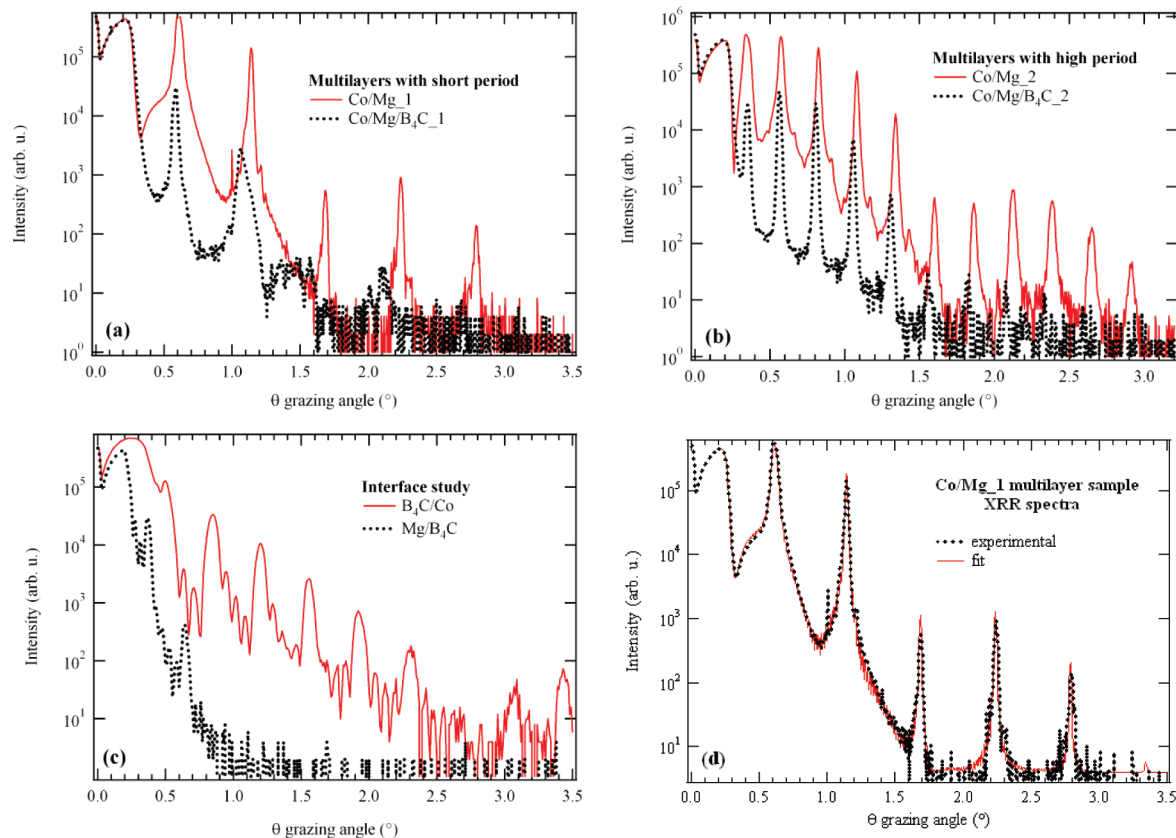


Figure 1. X-ray reflectivity curves measured at 0.154 nm: (a) Co/Mg₁ and Co/Mg/B₄C₁ samples; (b) Co/Mg₂ and Co/Mg/B₄C₂ samples; (c) B₄C/Co and Mg/B₄C multilayers deposited for thickness calibration purposes; and (d) fit of the reflectivity curve in the case of the Co/Mg₁ sample.

The Mg $K\beta$ spectrum of the Mg₂CoH₅ compound has been observed.³⁰ We expect the electronic structure (and hence the X-ray spectrum) of a magnesium-rich Mg–Co compound to be close to that of this hydride. However, it is not easy to compare this measured spectrum to ours owing to a discrepancy concerning the photon energy calibration and a problem of oxidation of the sample.

2.5. Nuclear Magnetic Resonance Spectroscopy. Zero field NMR has been performed with a homemade automated broadband NMR spectrometer. For the sake of sensitivity all the samples were measured at 4.2 K since the NMR signal increases as the inverse of the measurement temperature. All spectra have been recorded for different values of radio frequency field strengths allowing for correcting the NMR intensities with a frequency dependent enhancement factor. Therefore the NMR spectra represent the distribution of Co atoms versus their resonance frequency (i.e. the hyperfine field experienced by their nuclei).^{31,32} The NMR resonance frequency is sensitive to the local environment of the probed atoms: nearest neighbor local structure and/or local chemical environment.

Bulk reference samples consisting of 1% B and 1% Mg into Co have been measured to check the influence of the B and Mg neighborhood on the Co resonance frequency (hyperfine field). NMR lines at 117 and 170 MHz have been observed, respectively. According to the Co–B and Co–Mg phase diagrams, B and Mg do not mix easily with Co, therefore the observed NMR lines are likely to arise from Co₃B and Co₂Mg phases embedded into bulk Co.

3. Results and Discussion

3.1. X-ray Reflectivity at 0.154 nm. The reflectivity curves of the Co/Mg and Co/Mg/B₄C multilayers are presented in

Figure 1 on a logarithmic scale. In Figure 1a, five well-defined and narrow Bragg peaks are observed for the CoMg₁ sample up to 3°; on the contrary, in the case of the CoMgB₄C₁ sample, up to 3°, only the first Bragg peak is narrow and well-defined while the three following Bragg peaks are large and not intense. In Figure 1b, all the Bragg peaks are narrow and well-defined. For the Co/Mg/B₄C₂ sample, nine Bragg peaks are seen up to 2.5°, whereas eleven Bragg peaks are observed up to 3° for the Co/Mg₂ sample. The Bragg peaks are more intense for Co/Mg₂ with respect to Co/Mg/B₄C₂. It is also observed, Figure 1a and b, that the intensity of the background decreases more rapidly for Co/Mg/B₄C samples with respect to Co/Mg samples. From these curves, it appears that the structural quality of Co/Mg multilayers is better than that of Co/Mg/B₄C multilayers. The comparison of the reflectivity curves, with and without B₄C layers, gives evidence that the introduction of B₄C does not improve the structural quality of the multilayers. This is probably due to an interaction between the B₄C layers and the metal layers.

For the CoMg₁ and CoMgB₄C₁ samples, the position of the Bragg peaks leads to a period value equal to 7.92 and 8.40 nm, respectively (see Table 2). The correction for refraction is taken into account in the calculation. For the CoMg₂ and CoMgB₄C₂ samples, the position of the Bragg peaks corresponds to a period value equal to 16.70 and 17.13 nm, respectively (see Table 2). In the case of the Co/Mg₁ and Co/Mg₂ samples, a good agreement exists between the aimed and experimental period values (difference of about 1%). On the contrary, for the CoMgB₄C₁ and CoMgB₄C₂ samples, the difference between the aimed and experimental values becomes significant (between 5 and 6%). The introduction of a B₄C layer within the multilayer structure decreases the period

TABLE 2: Variation over 108 Days of the Period Values Calculated Using the Refraction Corrected Bragg Law and Parameter Values Extracted from the Fit of the Co/Mg_2 Reflectivity Curve Measured at 0.154 nm^a

sample	<i>d</i> (nm) period ^b		XRR fit			
	<i>t</i> = 0	<i>t</i> = 108 days	<i>d</i> _{Co} (nm); <i>d</i> _{Mg} (nm)	<i>d</i> (nm)	σ_{Co} (nm); σ_{Mg} (nm)	density ratios: Co (%); Mg (%)
CoMg_1	7.92	7.95	2.51; 5.44	7.95	0.56; 0.54	91 ± 5; 105 ± 5
CoMgB ₄ C_1	8.40	8.46	—	—	—	—
CoMg_2	16.70	16.71	2.63; 14.10	16.73	0.40; 0.40	102 ± 5; 100 ± 5
CoMgB ₄ C_2	17.13	17.17	—	—	—	—

^a σ stands for the interfacial roughness. Corrected for refraction. ^b The period is calculated using the Bragg law corrected from refraction.

value (period contraction) due to a reaction between the B₄C layer and the metal layer.

To identify which interface, B₄C/Co or Mg/B₄C, is responsible for the poor reflectivity of the Co/Mg/B₄C stack, we compare in Figure 1c the reflectivity curves of the B₄C/Co and Mg/B₄C multilayers made of only 5 or 10 periods and the designed period was 15 nm for both samples. These two multilayers were prepared in a preliminary batch by using nonoptimized conditions to calibrate the deposited thicknesses. It is clearly seen that the Mg/B₄C system leads to a very low reflectivity, only two very weak Bragg peaks being observed. The first Bragg peaks of the B₄C/Co system are also weak with respect to the plateau before the total reflection. The number of bilayers of B₄C/Co is 10 while that of Co/Mg is 30 and as a consequence, all the Bragg peaks of the B₄C/Co multilayer are about three times broader, Figure 1c, than those of Co/Mg and Co/Mg/B₄C multilayers, Figure 1a and b. These observations indicate that the optical qualities of both B₄C/Co and Mg/B₄C are low, the Mg/B₄C interface being the worse one. Therefore, interface imperfections, including roughness and/or diffuseness, greatly limit the final Co/Mg/B₄C multilayer reflectivity.

To estimate the time stability of these samples, we have checked the reproducibility of the reflectivity measurements over a period of 108 days: the corresponding periods are also presented in Table 2. The different period values coincide within the experimental uncertainty demonstrating the good time stability of the Co/Mg stack. It would be necessary to measure the reflectivity of the multilayers over even a larger period of time because applications require stability over a few years.

To improve the description of the multilayer, the Co/Mg_1 and Co/Mg_2 reflectivity curves are fitted in order to estimate the values of the structural parameters of the stack: the thickness, roughness, and density of the various layers. The roughness deduced from the fit is an overall roughness including the contributions from both geometrical roughness and interdiffusion. These values are collected in Table 2. In that table, the density ratio (%) is defined as the density of the layer divided by the density of the bulk. As an illustration, Figure 1d shows the comparison between the experimental and fitted XRR curve in the case of the Co/Mg_1 sample. We do not fit the reflectivity of the CoMgB₄C_1 and CoMgB₄C_2 samples because of the large number of parameters and the probable reaction of the B₄C layer with the metal layer.

The values of the Co and Mg layer thickness are those of the designed structure for CoMg_1 while for CoMg_2, a slight difference exists between these values: compared to the design, the Co layer is about 3% thicker and the Mg layer about 3% thinner. In both cases, the period values are close to that calculated with the Bragg law corrected for refraction. For a given sample, the roughness values at both interfaces are comparable. The density values are given within a 5% uncertainty. For both samples, the layers are as dense as the bulk materials, except in the CoMg_1 sample where the Co layer is

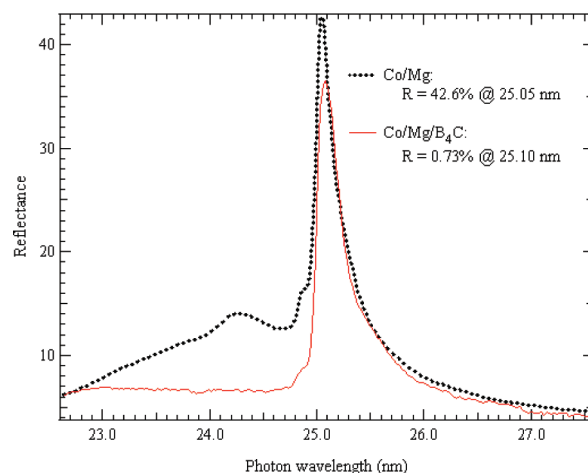


Figure 2. EUV reflectivity curves of the Co/Mg and Co/Mg/B₄C multilayers measured at 45°. The Co/Mg/B₄C curve is amplified 50 times.

less dense than in the bulk. As a summary, the fitting results indicate that the deposited multilayered samples coincide in a satisfactory manner with those expected in the preparation step.

3.2. EUV Reflectivity. The reflectivity curves of the CoMg_2 and CoMg/B₄C_2 multilayer samples measured at 45° and around the photon energy of 50 eV are presented in Figure 2 on a linear scale. The asymmetric shape of the two reflectivity curves is due to the presence of the Mg L₂ and L₃ edges at 49.78 and 49.50 eV respectively). Contrary to the CoMgB₄C_2 sample where, preceding the maximum value, the reflectivity remains constant, in the case of the CoMg_2 sample an additional structure centered around 24.3 nm (or 51 eV) is present.

The maximum of the CoMg_2 reflectivity curve is equal to 42.6% at 25.05 nm whereas that of the CoMgB₄C_2 sample is only 0.73% at 25.10 nm. In the case of the CoMg_2 sample, the measured value has to be compared to the simulated value (56.5% at 25.2 nm given an “ideal” multilayer: no interaction and no roughness at the interfaces). That is to say that the experimental value represents 75% of the simulated value, which is higher than in the case of the Mg/SiC system.⁷ Moreover, for comparison, using the parameter values extracted from the fit of the CoMg_2 XRR curve measured at 0.154 nm (see Table 2) for reflectivity simulations in the EUV range, the reflectivity of this multilayer is calculated to be 27% at 25.2 nm at 45° of grazing incidence. The absence of agreement between this latter value and the measured value reflects the fact that, in the fitting procedure, the values retained for the structural parameters (thickness, roughness, and density of the layers) are not correctly optimized.

In the case of the CoMgB₄C_2 sample, the measured reflectivity curve demonstrates the poor quality of the multilayer in terms of optical performances. The introduction of a B₄C material at the Co-on-Mg interface does not contribute at all to

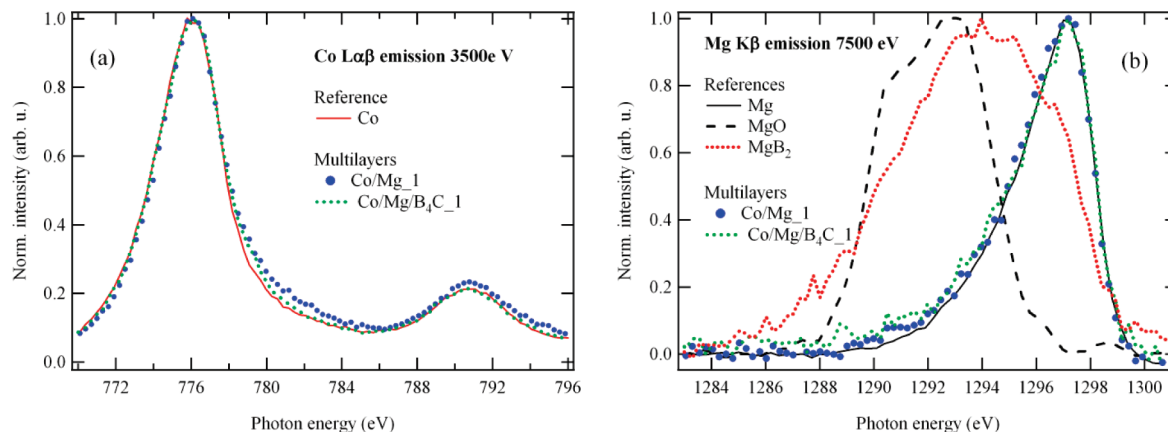


Figure 3. (a) Co $L\alpha\beta$ and (b) Mg $K\beta$ emission bands originating from the references (Co (a) and Mg, MgO, and MgB_2 (b)) compared to those of the Co/Mg_1 and Co/Mg/B₄C_1 multilayer samples.

improve the quality of the interfaces, in contrast with the IMD simulations for an “ideal” multilayer (see Table 1). A reaction between the B₄C layer and the metallic layers could be responsible for this drastic drop of the reflectivity with respect to the Co/Mg system.

3.3. XES Analysis. The Co $L\alpha\beta$ emission spectrum originating from the Co reference is compared to that of the CoMg_1 and CoMgB₄C_1 multilayer samples in Figure 3a while the Mg $K\beta$ emission spectrum originating from the references (Mg, MgO, and MgB_2) is compared to that of the CoMg_1 and CoMg/B₄C_1 multilayer samples in Figure 3b.

Concerning the Co $L\alpha\beta$ emission, Figure 3a, the spectra of the multilayers is close to that of the Co reference sample. From one sample to the other, the position of the Co $L\alpha$ maximum does not vary by more than 0.3 eV. The position of the Co $L\beta$ maximum remains constant for the three samples. The intensity ratio determined with the values of the maximum of the Co $L\alpha$ and $L\beta$ emission bands remains of the order of 0.2 for the three samples. As a consequence, the Co $L\alpha\beta$ emission band shapes are not sufficiently different from each other to enable us to discuss the formation of interfacial compounds between successive layers within the multilayers. The Co $L\alpha\beta$ emission is not sensitive enough to the physicochemical environment surrounding the emitting Co atoms. Our XES analysis will be essentially based on Mg $K\beta$ experimental data.

For the Mg $K\beta$ emission, Figure 3b, the multilayers spectra are rather similar to that of the Mg reference. Thus, this result allows us to say that, within the CoMg_1 and CoMgB₄C_1 samples, the Mg atoms are in a physicochemical state close to that of Mg atoms in the Mg metallic state. Nevertheless, we can try to gain further insight into the comparison of these spectra. In the high photon energy side, the multilayer spectra are both close to that of the Mg reference. On the contrary, in the low photon energy side, the shape of the multilayer spectra slightly differs from that of the Mg reference: a kind of tail is observed in the region where the respective maxima of the MgO and MgB_2 Mg $K\beta$ emission spectra are present (1293 eV for MgO and 1294 eV for MgB_2). To infer the possible oxidation of the Mg atoms present within the multilayer, it is advisable to decrease the energy of the incident electrons: the analyzed depth becomes thinner and information about the layers close to the surface is provided.

In Figure 4 we study in the case of the CoMg_1 sample the change, as a function of the electron energy, of the shape of the Mg $K\beta$ emission band. For an electron energy equal to 4.5 keV, the analyzed depth is estimated, using CASINO software,³³ to correspond to the 20 first Mg layers in Co/Mg, and recovers

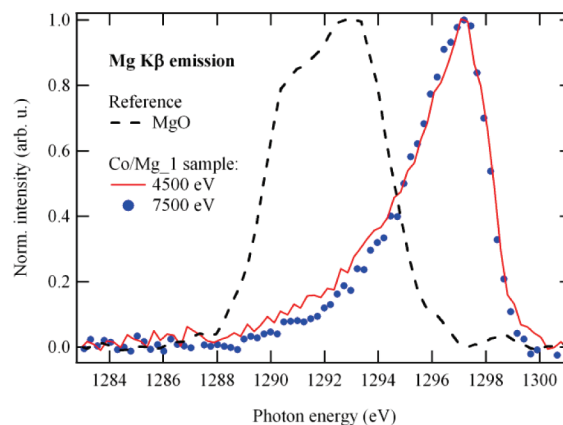


Figure 4. Change, as a function of the electron energy, of the shape of the Mg $K\beta$ emission band originating from the Co/Mg_1 sample, compared to that of the MgO reference.

the all 30 Mg layers at 7.5 keV of electron energy. The tail observed in the Mg $K\beta$ emission spectrum is more intense with electrons of energy equal to 4.5 keV. The same effect is also observed in the CoMgB₄C_1 sample (not shown). Thus the Mg atoms present within the two multilayers are slightly oxidized. In the case of the CoMgB₄C_1 sample, this result does not allow us to exclude that the Mg atoms can also slightly react with B atoms to form the MgB_2 compound.

Another explanation for the tail observed in the spectrum of the CoMg_1 sample could be that a Co–Mg compound forms at the interfaces of the multilayer. Indeed the experimental spectrum of $MgCo_2$ is not published and one could imagine that its maximum appears in the same region of the tail as that of MgO. We present in Figure 5 the Mg $K\beta$ spectrum of the Mg and $MgCo_2$ compounds calculated from the first principles using the Wien2k software³⁴ compared to the experimental one originating from the Mg reference sample. The calculated spectrum is obtained from the Mg 3p density of states weighed by the transition probability and convoluted by a Lorentzian function to take into account the natural width of the Mg 1s level and by a Gaussian function to take into account the experimental broadening. The comparison for Mg metal shows that the calculation reproduces quite accurately the experiment. All the spectra are presented on an energy scale relative to the position of the Fermi level. The energy position of the maximum of the $MgCo_2$ emission band is about 0.4 eV higher than that of the Mg spectrum. More striking is the large width of the Mg emission band with respect to that of $MgCo_2$. From these calculations, we can affirm that, within our sensitivity, the

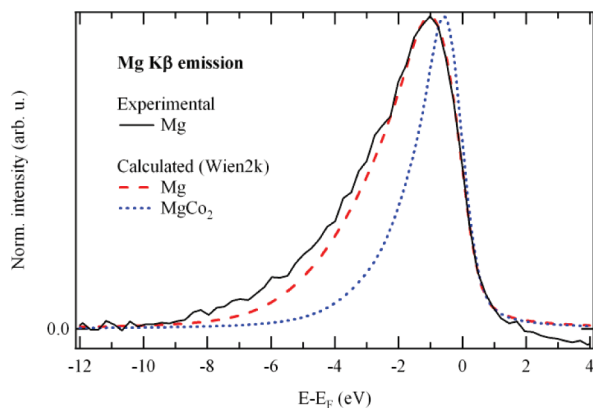


Figure 5. Comparison of the Mg $K\beta$ emission band calculated for the Mg and $MgCo_2$ compounds by using Wien2k with that measured at 7500 V for the Mg reference sample. The energy scale refers to the position of the Fermi level E_F .

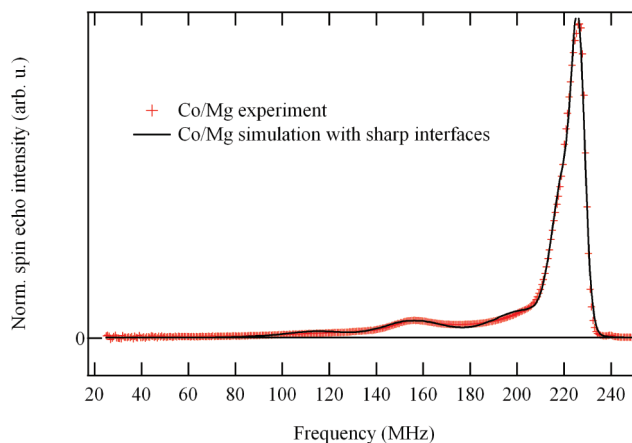


Figure 7. Simulation of the Co/Mg multilayer spectrum with a sharp interface model.

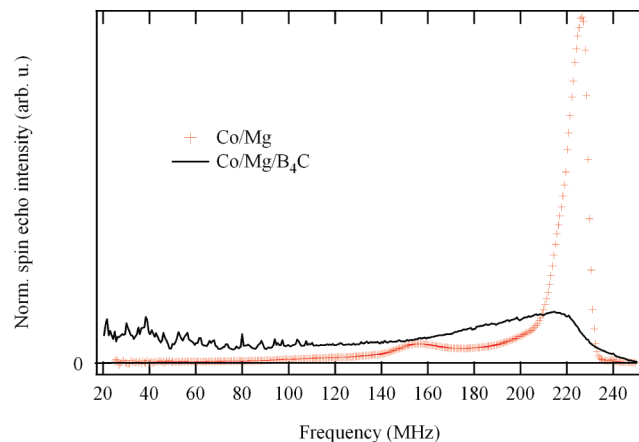


Figure 6. NMR spectra of Co/Mg and Co/Mg/ B_4C multilayers. The spectra surface areas are normalized to the same area.

possible formation of the $MgCo_2$ compound at the interfaces of the CoMg_1 and CoMg B_4C _1 samples is not confirmed by XES. From comparison with transition metal silicides,³⁵ the same kind of narrow bandwidth spectrum is expected for other possible Co–Mg compounds that could form out of equilibrium: $CoMg^{36,37}$ or $CoMg_2^{37,38}$

3.4. NMR Analysis. NMR spectra obtained for the Co/Mg and Co/Mg/ B_4C multilayers are presented in Figure 6. To compare the shape of the spectra, their total surface area is normalized to one. The thickness of the Mg layers has no influence on the NMR spectra (neither in shape nor in intensity) and therefore on the sample structure; for the sake of clarity one spectrum only of each type of sample is shown.

As can be seen, the shape of the spectra of the two kinds of samples is very different. The Co/Mg samples show a well-defined line at 226 MHz that is the fingerprint of bulk hcp Co. The Co atoms are mainly situated in pure Co layers and the intermixing at the Co/Mg interfaces is limited. An additional line is observed at 156 MHz. This line is at a frequency significantly different from the one observed for the CoMg1% reference sample (170 MHz) and has very probably a different origin. Actually the shape of the low-frequency part of the spectrum (below 210 MHz) looks very similar to the shape observed in multilayers with sharp interfaces,^{31,32} but this interpretation is difficult to ascertain because of the lack of appropriate reference samples. However a tentative simulation with the step interface model³⁹ that is appropriate for samples with sharp interfaces is presented in Figure 7. The model

reproduces closely the experimental spectrum. It must be noted that in this model the ratio between the intensities of the interfacial part of the spectrum and the bulk part of the spectrum is not an adjusted parameter, but is fixed from the thickness of the deposited Co layers. This gives us confidence in our interpretation and suggests strongly that the Co/Mg multilayers present sharp interfaces.

In contrast, the shape of the Co/Mg/ B_4C spectra is very different. No Co bulk line is observed anymore. This shows that the Co layers are not pure but that alien atoms (Mg, B, or C) are mixed with Co. Since the Co/Mg multilayers show sharp interfaces the mixing is likely to originate from the Co/ B_4C interfaces. The intermixing in the Co/Mg/ B_4C is more important than the one depicted by the change in spectra shape since the absolute integral intensity of the Co/Mg/ B_4C spectra is 3 times smaller than the intensity of the Co/Mg spectra. This means that two-thirds of the total Co atoms included in these samples are not observed in the Co/Mg/ B_4C NMR spectra. These Co atoms are most probably situated into non-ferromagnetic phases (and therefore give no NMR signal) with a large content of Mg, B, or C atoms. This confirms the large mixing observed by XRR in the Co/Mg/ B_4C samples.

The samples have been analyzed after a period of three months where they were stocked in a desiccator. No significant variation of the NMR signal is detected for both Co/Mg and Co/Mg/ B_4C systems. This confirms the reflectivity measurement in the hard X-ray range after 108 days for the Co/Mg multilayer.

4. Conclusion

The Co/Mg multilayers are promising for applications in the EUV range around 25 nm. A reflectivity of 46% at 45° angle is measured representing three-quarters of the ideal reflectivity, i.e. for a perfect multilayer without roughness and interdiffusion. This experimental value can be improved by increasing the number of bilayers within the stack and also by optimizing the deposition conditions and the capping layer. Thus, it is important to characterize in detail these kinds of nanometric multilayers. This was done in the present work by using X-ray reflectivity in the hard and soft X-ray ranges, X-ray emission spectroscopy, and nuclear magnetic resonance spectroscopy. The reflectivity measurements and their fit enable us to establish that the thicknesses of the various deposited layers are close to the aimed ones during the preparation. It was also deduced from these measurements that the interfacial roughness is less than 0.5 nm. XES and NMR spectra permit the determination of the chemical state of the Mg and Co atoms, respectively, at the interfaces.

They reveal no compound formation and abrupt interfaces. Thus the difference between the experimental and simulated reflectivity values can be ascribed to the interfacial roughness.

The introduction of thin boron carbide interfacial layers into the stack considerably degrades the EUV reflectance, leading to a poor value of less than 1%. From XES and NMR measurements, it is observed that it is the Co atoms that react with the B or C atoms of the carbide layers to form an interfacial compound while the Mg atoms seem undisturbed. It has not been possible to determine this compound due to the lack of reference compounds. We have shown that the Mg/B₄C system is worse (in terms of optical qualities) than the Co/B₄C system. From this simple fact, we could have deduced that within the trilayer, the Mg/B₄C interfaces were responsible of the very low reflectivity. However, this is not the case. From XES and NMR, we determine that it is the Co/B₄C interfaces that lead to the deterioration of the reflectivity. In fact within the multilayer, there is a competition between the Co and Mg atoms to react with the atoms of the B₄C layers and it appears that in the stack, the Co atoms are more reactive than the Mg ones. Thus, it is not possible to infer the properties of a trilayer system from the properties of bilayer systems.

The temporal stability of the Co/Mg and Co/Mg/B₄C multilayers has been checked over a period of about three months and reveals no significant deterioration of the reflectivity in the hard X-ray range as well as of the NMR signal. For applications, this stability has to be checked over longer periods of time. The thermal stability must be verified because the multilayers can be subjected to high thermal loads. In this case, it probably will be necessary to consider the introduction of an efficient diffusion barrier. This will be addressed in a forthcoming paper.

Acknowledgment. S. Nannarone, A. Giglia, and N. Mahne from the BEAR beamline at the ELETTRA synchrotron are thanked for their help during the measurements of EUV reflectivity. The authors from Tongji University are indebted to the National Natural Science Foundation of China (Granted No. 10825521).

References and Notes

- (1) Yanagihara, M.; Yamashita, K. X-ray Optics. In *X-Ray Spectrometry: Recent Technological Advances*; Tsuji, K., Injuk, J., van Grieken, R., Eds.; John Wiley & Sons: Chichester, UK, 2004.
- (2) PXRMS Multilayer Survey Results, <http://henke.lbl.gov/cgi-bin/mldata.pl>.
- (3) Windt, D. L. *Comput. Phys.* **1998**, *12*, 360.
- (4) Hu, M.-H.; Le Guen, K.; André, J.-M.; Jonnard, P.; Zhou, S. K.; Li, Ch.; Zhu, J. T.; Wang, Z. S. *AIP Conf. Proc.* 1221 (ICXOM 20, 2009).
- (5) Braun, S.; Mai, H.; Moss, M.; Scholtz, R.; Leson, A. *Jpn. J. Appl. Phys.* **2002**, *41*, 4074.
- (6) Maury, H.; Jonnard, P.; André, J.-M.; Gautier, J.; Roulliay, M.; Bridou, F.; Delmotte, F.; Ravet, M.-F.; Jérôme, A.; Holliger, P. *Thin Solid Films* **2006**, *514*, 278.
- (7) Maury, H.; Jonnard, P.; Le Guen, K.; André, J.-M.; Wang, Z.; Zhu, J.; Dong, J.; Zhang, Z.; Bridou, F.; Delmotte, F.; Hecquet, C.; Mahne, N.; Giglia, A.; Nannarone, S. *Eur. Phys. J. B* **2008**, *64*, 193.
- (8) Windt, D. L.; Bellotti, J. A. *Appl. Opt.* **2009**, *48*, 4932.
- (9) Zhu, J.; Zhou, S.; Li H.; Huang, Q.; Wang, Z.; Le Guen, K.; Hu, M.-H.; André, J.-M.; Jonnard, P. *Opt. Express*. Submitted for publication.
- (10) Gautier, J.; Delmotte, F.; Roulliay, M.; Bridou, F.; Ravet, M.-F.; Jérôme, A. *Appl. Opt.* **2005**, *44*, 384.
- (11) Wormington, M.; Panaccione, C.; Matney, K.; Bowen, D. *Phil. Trans. R. Soc. London, Part A* **1998**, *357*, 2827.
- (12) Nannarone, S.; Borgatti, F.; DeLuisa, A.; Doyle, B. P.; Gazzadi, G. C.; Giglia, A.; Finetti, P.; Mahne, N.; Pasquali, L.; Pedio, M.; Selvaggi, G.; Naletto, G.; Pelizzo, M. G.; Tondello, G. *AIP Conf. Proc.* **2004**, *708*, 450.
- (13) Bonnelle, C.; Vergand, F.; Jonnard, P.; André, J.-M.; Staub, P. F.; Avila, P.; Chargelègue, P.; Fontaine, M.-F.; Laporte, D.; Paquier, P.; Ringuet, A.; Rodriguez, B. *Rev. Sci. Instrum.* **1994**, *65*, 3466.
- (14) Jonnard, P.; Vergand, F.; Bonnelle, C.; Orgaz, E.; Gupta, M. *Phys. Rev. B: Condens. Matter Mater. Phys.* **1998**, *57*, 12111.
- (15) Azaroff, L. V. *X-ray Spectroscopy*; McGraw-Hill Inc.: New York, 1974.
- (16) Bonnelle, C. *Annu. Rep. Prog. Chem., Sect. C: Phys. Chem.* **1987**, *84*, 201.
- (17) Iwami, M.; Kusaka, M.; Hirai, M.; Tagami, R.; Nakamura, H.; Watabe, H. *Appl. Surf. Sci.* **1997**, *117*, 434.
- (18) Kurmaev, E. Z.; Galakhov, V. R.; Shamin, S. N. *Crit. Rev. Solid State Mater. Sci.* **1998**, *23*, 65.
- (19) Miyata, N.; Ishikawa, S.; Yanagihara, M.; Watanabe, M. *Jpn. J. Appl. Phys. Part 1* **1999**, *38*, 6476.
- (20) Jarrige, I.; Jonnard, P.; Frantz-Rodriguez, N.; Danaie, K.; Bosseboeuf, A. *Surf. Interface Anal.* **2002**, *34*, 694.
- (21) Galakhov, V. R. *X-Ray Spectrom.* **2002**, *31*, 203.
- (22) Salou, M.; Rioual, S.; Ben Youssef, J.; Dekadjevi, D. T.; Pogossian, S. P.; Jonnard, P.; Le Guen, K.; Gamblin, G.; Rouvellou, B. *Surf. Interface Anal.* **2008**, *40*, 1318.
- (23) Le Guen, K.; Gamblin, G.; Jonnard, P.; Salou, M.; Ben Youssef, J.; Rioual, S.; Rouvellou, B. *Eur. Phys. J.: Appl. Phys.* **2009**, *45*, 20502.
- (24) Maury, H.; André, J.-M.; Le Guen, K.; Mahne, N.; Giglia, A.; Nannarone, S.; Bridou, F.; Delmotte, F.; Jonnard, P. *Surf. Sci.* **2009**, *603*, 407.
- (25) Ohtani, H.; Hasebe, M.; Nishizawa, T. *Trans. Iron Steel Inst. Jpn.* **1984**, *24*, 857.
- (26) Faria, M. I. S. T.; Leonardi, T.; Coelho, G. C.; Nunes, C. A.; Avillez, R. R. *Mater. Charact.* **2007**, *58*, 358.
- (27) *Landolt-Börnstein*, New Series IV/5, subvolume C; Springer-Verlag: New York, 1993.
- (28) Nayeb-Hashemi, A. A.; Clark, J. B. *Phase Diagrams of Binary Magnesium Alloys*; ASM International: Metals Park, OH, 1988; pp 43–46.
- (29) Jonnard, P.; Le Guen, K.; Gauvin, R.; Le Berre, J.-F. *Microsc. Microanal.* **2009**, *15*, 36.
- (30) Belin, E.; Gupta, M.; Zolliker, P.; Yvon, K. *J. Less-Common Met.* **1987**, *130*, 267.
- (31) Meny, C.; Panissod, P. *Modern Magnetic Resonance*; Webb, G., Ed.; Springer: Heidelberg, Germany, 2006.
- (32) Panissod, P.; Meny, C. *Appl. Magn. Reson.* **2000**, *19*, 447.
- (33) Hovington, P.; Drouin, D.; Gauvin, R. *Scanning* **1997**, *19*, 1. Drouin, D.; Hovington, P.; Gauvin, R. *Scanning* **1997**, *19*, 20. Hovington, P.; Drouin, D.; Gauvin, R.; Joy, D. C.; Evans, N. *Scanning* **1997**, *19*, 29.
- (34) Schwarz, K.; Blaha, P. *Comput. Mater. Sci.* **2003**, *28*, 259.
- (35) Jarrige, I.; Capron, N.; Jonnard, P. *Phys. Rev. B* **2009**, *79*, 035117.
- (36) Yoshida, M.; Bonhomme, F.; Yvon, K.; Fischer, P. *J. Alloys Compd.* **1993**, *190*, L45.
- (37) Gennari, F. C.; Castro, F. J. *J. Alloys Compd.* **2005**, *396*, 182.
- (38) Wang, Y. J.; Aizawa, T.; Nishimura, C. *Mater. Trans.* **2006**, *47*, 1052.
- (39) Meny, C.; Panissod, P.; Loloee, R. *Phys. Rev. B* **1992**, *45*, 12269.